Journal of Molecular Liquids 269 (2018) 796–804

Contents lists available at ScienceDirect

Journal of Molecular Liquids

journal homepage: www.elsevier.com/locate/molliq

An intermittent amyloid phase found in gemini (G5 and G6) surfactant induced β-sheet to α-helix transition in concanavalin A protein

Javed Masood Khan [a,*], Mohammad Rizwan Khan [b], Priyankar Sen [c], Ajamaluddin Malik [d], Mohammad Irfan [e], Rizwan Hasan Khan [f,**]

[a] Department of Food Science and Nutrition, Faculty of Food and Agricultural Sciences, King Saud University, 2460, Riyadh 11451, Saudi Arabia
[b] Department of Chemistry, College of Science, King Saud University, P.O. Box 2455, Riyadh 11451, Saudi Arabia
[c] Centre for Bioseparation Technology, VIT University, Vellore 632014, India
[d] Protein Research Chair, Department of Biochemistry, College of Science, King Saud University, Riyadh, Saudi Arabia
[e] National Institute of Plant Genomic Research, Aruna Asaf Ali Marg, New Delhi 110067, India
[f] Molecular Biophysics and Biophysical Chemistry Group, Interdisciplinary Biotechnology Unit, Aligarh Muslim University, Aligarh 202002, India

ARTICLE INFO

Article history:
Received 25 February 2018
Received in revised form 10 May 2018
Accepted 15 August 2018
Available online 18 August 2018

Keywords:
Lectin
Concanavalin A
CTAB
Gemini surfactant
Amyloid fibril and β to α transition

ABSTRACT

Surfactant-induced amyloid fibrillation has many implications in laboratory and industry. Previously, cetyltrimethylammonium bromide (CTAB; $C_{19}H_{42}BrN$) induced amyloid formation in concanavalin A (ConA) has been reported by authors (Khan, JM et al., 2016 A). In this work, cationic gemini surfactants pentanediyl 1,5 bis (dimethylcetylammonium bromide); 16-5-16 (G5), and hexanediyl 1,6 bis (dimethyl cetyl ammonium bromide); 16-6-16 (G6) were found to induce amyloid-like aggregation in ConA as studied with turbidity at 350 nm, Rayleigh scattering and Thioflavin T (ThT) binding assay and Far UV CD. The sizes of the aggregates were characterized with dynamic light scattering (DLS) and atomic force microscopy (AFM). Hydrodynamic radii (*Rh*) of the aggregates were found to be 74 nm and 122 nm with 50 μM of G5 and G6 respectively. Even at 7.5 μM, gemini surfactants seems disrupting hydrophobic pockets of ConA and result in aggregation. On the contrary, aggregation disappeared around 250 μM surfactant concentration with β-sheet → α-helix transition. The re-establishment of intra-molecular hydrogen bonding may have resulted in the formation of non-native α-helical structures. Alcohols, predominantly 2,2,2 trifuloroethanol (TFE), have been reported to induce α-helices in β-sheet proteins by solvent engineering. There are very few reports of β-sheet to α-helix transition induced by non-alcoholic substances. Our lab is pioneer in reporting surfactant (CTAB) induced β-sheet to α-helix transition in ConA (Khan, JM et al., 2016 A). This is the first report of G5 and G6 gemini surfactant induced β-sheet to α-helix transition, as per our knowledge. ConA being apoptotic to cancerous cells and having potential therapeutic effect on hepatoma, the observations done in this work could be of immense interest in vesicular delivery of ConA.

© 2018 Elsevier B.V. All rights reserved.

1. Introduction

Almost more than 50 types of diseases are now discovered which are directly connected to protein or peptide misfolding [1,2]. To understand the mechanism of protein or peptide misfolding is important for advancing protein science and prevention of such types of diseases. Some of the well-known protein misfolding diseases are Alzheimer's, Parkinson's, Huntington's, type II diabetes etc. [3]. The misfolded protein can form ordered structures; known as amyloid fibrils, and can be characterized by cross β-sheet assemblies. Every strands of amyloid fibril run perpendicular to the long axis of fibril [4]. Amyloid fibril forms under non-native conditions and partially unfolded states of proteins are more prone to aggregate and form amyloid fibril [5]. The partially unfolded states can be generated under in vitro conditions also. The temperature and pH are factors to induce partially unfolded states in proteins [6]. Generally, amyloid fibril formation is a stepwise process comprising oligomerization, nucleation and growth phase [7]. Sometimes, amyloid fibrils are formed without the formation of nucleus [8]. It is known that only external factors or ligand can reduced the length of nucleation [9]. Several chemical entities, for example lipids and surfactants are also known to promote amyloid-like fibrils in proteins

Abbreviations: ThT, Thioflavin-T; ConA, concanavalin A; AFM, atomic force microscopy; DLS, dynamic light scattering; CD, circular dichroism; CMC, critical micellar concentration.

* Correspondence to: J. M. Khan, Department of Food Science and Nutrition, Faculty of Food and Agricultural Sciences, King Saud University, 2460, Riyadh 11451, Saudi Arabia.
** Correspondence to: R. H. Khan, Interdisciplinary Biotechnology Unit, Aligarh Muslim University, Aligarh, India.
E-mail addresses: javedjmk@gmail.com (J.M. Khan), rizwanhkhan1@gmail.com (R.H. Khan).

https://doi.org/10.1016/j.molliq.2018.08.092
0167-7322/© 2018 Elsevier B.V. All rights reserved.

[10,11]. Among surfactants, only anionic and cationic surfactants are found to induce amyloid fibrils [12,13]. Cetyltrimethyl ammonium bromide (CTAB) is cationic surfactant having positively charged head and hydrophobic tail. Cationic surfactant is promoting fibrillation in hen egg white lysozyme at alkaline pH [12]. The CTAB interacted electrostatically with aspartic and glutamic acids residues of protein at physiological pH and assisting amyloid fibril formation [14]. The cationic surfactant favor amyloid fibril formation below its critical micellar concentration (CMC) and no amyloid fibril was formed at above CMC in stem bromelain protein [15]. Apart from conventional surfactant, a gemini surfactant has also a great ability to induce amyloid-like fibril in proteins [16]. Gemini surfactant is unique in nature compared to conventional surfactant because gemini possess two positively charged hydrophilic head and two hydrophobic tail and both the chains are covalently linked with few carbon spacer group shown in Fig. 1. The gemini surfactant have very strong interacting property to the protein [17,18]. Geminis surfactant are surface-active agents and have strong propensity to form micelles at lower concentrations compared to conventional one and micellar concentration lies between the micro to millimolar which is depending on alkyl chains length [19–21]. Gemini surfactant is superior to the other conventional single-chain surfactants in terms of low Krafft temperature, CMC and high hydrophobic microdomain. Currently, geminis (m-E2-m) surfactants are getting more attention than conventional m-s-m type surfactants because of their easily cleavable, biodegradability and lower toxicity.

It is reported that low concentrations of gemini surfactant induces amyloid-like aggregates in β(1–40) peptides [22]. It is important to elucidate the effect of the gemini surfactant on the dynamics of protein fibrillogenesis. For this, we have tried to explore the mechanism of amyloid fibrillation induces by gemini surfactants on a plant lectin ConA.

Lectins are carbohydrate binding protein and highly specific for sugar moieties [23]. ConA is a legume lectin; extracted from jack-bean. It strongly agglutinates erythrocytes irrespective of blood-group, and various cancerous cells. It has an affinity for terminal α D mannosyl and α D glucosyl residues. Ca^{2+} and Mn^{2+} ions are required for its activity. It is a homotetramer protein at physiological pH, made up of 237 amino acid residues, predominantly β sheet secondary structure and isoelectric point (pI) ranges from 4.5 to 5.5 [24]. It dissociates into dimers at pH 5.6 or below. Between pH 5.8 and pH 7.0, ConA exists as a tetramer; above pH 7.0 higher aggregates are formed. It exhibits mitogenic activity which depends on its degree of aggregation. Its succinylation results in an active dimeric form which remains a dimer above pH 5.6. ConA does not have disulphide bond and its tertiary structure is flexible [25]. The monomer of ConA is almost 26.0 kDa, and its tertiary structure has been called as a "jellyroll" motif. Each sub units has a single sugar binding and two metal binding sites [26]. The structure of ConA is remarkably similar to human serum amyloid protein (SAP) that has a high affinity to amyloid fibrils and ubiquitously found in all kind of amyloid deposits [27]. ConA aggregates morphology dependent on solution pH and temperature. It is evident from already published report that form amyloid-like aggregates at pH 8.9 and amorphous aggregates at pH 5.1 at high temperature [28], and amyloid fibril in a non-nucleated manner at basic pH at 37 °C [29].

In this work, we have used several biophysical techniques to evaluate the role of gemini surfactant homologues ($C_{16}CsC_{16}Br_2$, where s = 5 and 6) on fibrillation of ConA protein. The role of spacer length of gemini was also tested in ConA amyloid fibrillation. Over all this study will help us to understand the molecular mechanism of G5 and G6 gemini surfactant induced amyloid fibrillation.

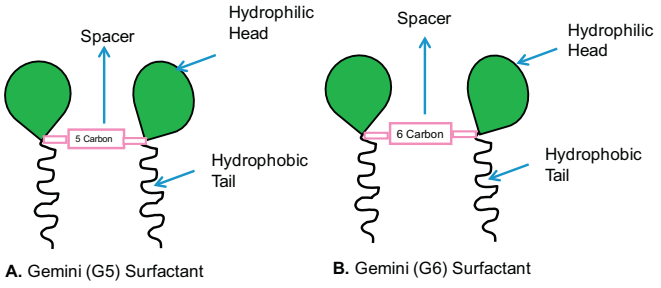

Fig. 1. Molecular structures of gemini surfactants: (A) G5 and (B) G6.

2. Experimental

2.1. Materials

Concanavalin A (ConA), Tris–HCl, and Thioflavin-T (ThT) were procured from Sigma Chemicals Co. (St. Louis, MO, USA). Other chemicals were used of analytical grade. The gemini surfactant bis (cetyldimethylammonium)butane dibromide, $C_{16}H_{33}(CH_3)2N^{+}–(CH_2)_s–N^{+}(CH_3)_2C_{16}H_{33}\cdot 2Br^{-}$, (where s = 5 and 6) were taken from Aijaz Ahmad Dar lab and they have synthesized and characterized according to already reported methods [30].

2.2. Protein concentration calculation

ConA was dissolved in 20 mM Tris buffer, pH 7.4. The concentrations of ConA were calculated by taking optical density at 280 nm. The optical density was taken on Perkin Elmer (Lambda25) spectrophotometer, by using molar extinction coefficients, $E^{1\%}_{1/4} = 11.4$ at 280 nm. ConA purity was checked by SDS-PAGE and data are provided as a Supplementary material (Fig. S1).

2.3. Turbidity measurements

Turbidity measurements were performed on Perkin-Elmer double beam UV–vis spectrophotometer. The ConA treated with and without G5 and G6 gemini surfactant (0–1500 μM) was quantified by taking absorbance at 350 nm at pH 7.4. As a control, the absorbance was also measured sample, which was containing similar concentration of G5 and G6 only. All the samples were incubated overnight before measurements.

2.4. Light scattering

Light scattering was carried out on Hitachi F-7000 fluorescence spectrofluorometer. The light scattering was done to identify the ConA aggregates in the solutions. The ConA alone and with various concentrations of G5 and G6 (0–1500 μM) gemini surfactants was excited at 350 nm and emission was recorded at 350 nm wavelength at pH 7.4. The light scattering at 350 nm was plotted against different concentrations of G5 and G6 surfactants. The excitation and emission slit widths were kept constant 2.5 nm in all the measurements. The ConA concentration was fixed 0.2 mg ml^{-1} in all the samples. Prior RLS measurements, all the samples treated with G5 and G6 were incubated overnight at room temperature.

2.5. DLS measurements

DynaPro-TC-04 (Wyatt Corporation) instruments were used which were equipped with temperature controller micro sampler. The ConA stock and G5 and G6 surfactant stocks were centrifuge at 5000 rpm for 10 min and then the supernatant was filtered through 0.22 μm syringe filter. After filtration, ConA (1.0 mg ml^{-1})was treated with and without different concentrations of G5 and G6 surfactants at pH 7.4. Every sample was scanned 60 times, and then average was taken. The obtained data was analyzed by Dynamic 610.0.10 software. The mean hydrodynamic radii (*Rh*) and polydispersity (Pd) were

assessed from an autocorrelation analysis of scattered light intensity based on the translational diffusion coefficient from the Stokes–Einstein equation

$$Rh = \frac{kT}{6\pi\eta D^{25\ 0C}_{W}}$$

where *Rh* is the hydrodynamic radius, k is the Boltzmann's constant, T is the absolute temperature, η is the viscosity of water and D is the translational diffusion coefficient.

2.6. ThT assay

ThT fluorescence assay was done to distinguish aggregates structures. The ThT was added to all the samples of ConA with or without 2.5, 12.5, 25.0, 50.0 and 75.0 μM of G5 and G6 surfactant. After addition of ThT the samples were further incubated for 20 min. The ThT fluorescence emission spectra were recorded at room temperature. The samples were excited at 440 nm and emission spectra were collected in the range of 470–600 nm wavelength. ThT concentrations were also calculated by taking absorbance at 440 nm by using extinction coefficient 36,000 M^{-1} cm^{-1}.

2.7. Circular dichroism spectroscopy

Far-UV CD spectropolarimeter is used to identify the secondary structural changes in ConA protein in response to G5 and G6 gemini surfactant. The far-UV CD spectra of ConA with and without of G5 and G6 were scanned on Jasco J-815 circular dichroism (CD) spectropolarimeter. The far-UV CD spectra were scanned in the range of 200–260 nm with a difference of 1 nm. Quartz cuvette with 0.1-cm path length was used. The ConA was treated with G5 and G6 gemini surfactant (12.5, 25.0, 37.5, 50.0, 75.0, 250.0 and 500.0 μM) at pH 7.4 buffer. The far-UV CD spectra of all the samples were taken on the average of three scans. The far-UV CD results were expressed as mean residual ellipticity and defined as.

$$\mathrm{MRE} = \Theta_{obs}\ (\mathrm{mdeg})/10 \times n \times Cp \times l$$

where θ_{obs} is the CD in millidegrees, n is the number of amino acid residues of the protein, l is the path length of the cell in centimeters and Cp is the molar fraction of proteins. The K2D2 on line server was used to quantitate the percent secondary structural change in ConA with G5 and G6 gemini surfactant.

2.8. Atomic force microscopy (AFM)

AFM was utilized to distinguish the morphology of gemini-induced aggregates. The ConA (0.2 mg ml^{-1}) was treated with 50.0 μM of G5 and G6 gemini surfactant at pH 7.4 and incubate for overnight. The incubated samples were further diluted two times and then few drops of diluted samples were placed on the freshly prepared mica surface. After 15 min, the mica was rigorously washed with Milli-Q water. After washing the mica was left for several h for drying. After dryness, AFM imaging was carried out on Bioscope Catalyst AFM (Bruker, USA) in the tapping mode. The AFM images were processed for publication with the use of Nanoscope Analysis v.1.4 software.

3. Results

3.1. Turbidity measurements

The turbidity study at 350 nm is a measure of protein aggregation [2,3,5–8]. Gemini Surfactant (G5 and G6) induced aggregation of ConA was examined by taking turbidity at 350 nm. The change in turbidity of ConA at pH 7.4 incubated with different concentration (0–1500 μM) of G5 and G6 gemini surfactants are shown in Fig. 2A. Baseline turbidity was found when ConA was incubated without gemini surfactants. The turbidity was start appearing with the presence of 7.5 μM gemini surfactants and maximum turbidity was seen with 50 μM of the gemini surfactants. Beyond 250 μM of surfactants turbidity suddenly disappears. The intensity of turbidity was found to be more in case of G6 compared to G5 gemini surfactant. The turbidity results are indicating that the micromolar concentrations of the gemini surfactants are promoting aggregation in ConA at pH 7.4.

3.2. Rayleigh scattering measurements

Rayleigh scattering is also used to characterize protein aggregation. In Fig. 2B, showed the effect of G5 and G6 gemini surfactant on ConA protein at physiological pH. No scattering at 350 nm was observed in ConA without gemini surfactants at pH 7.4. However, in the presence of the both the surfactants scattering was increased exponentially. The scattering start from 7.5 μM and reached maximum at 50 μM of the gemini surfactants. The decrease in scattering was also recorded with further increase in gemini surfactant concentrations (250–1500 μM). Interestingly, scattering was disappeared above 250 μM surfactant concentration. The data further support our hypothesis that the ConA form aggregates due to exposure of low concentrations of G5 and G6 gemini surfactant and aggregation disappeared in the presence higher surfactant concentrations. The light scattering of samples containing both the gemini surfactants alone at pH 7.4 was also measured as a

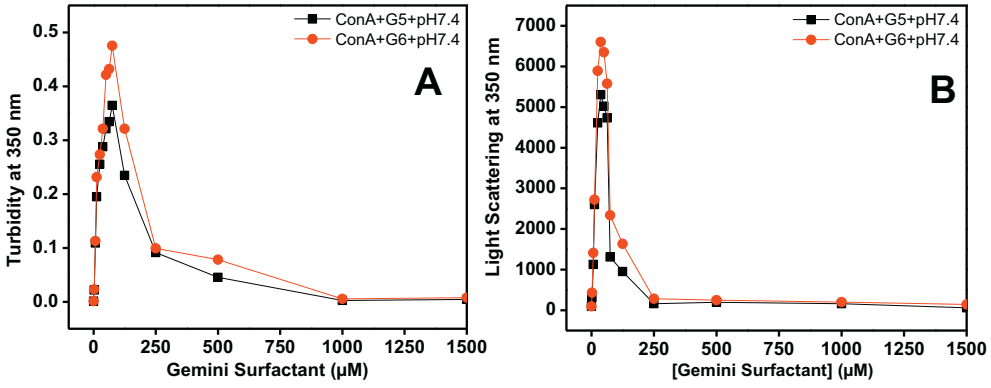

Fig. 2. Turbidity (A) and Rayleigh Light Scattering (RLS) (B) measurement of samples by taking absorbance and fluorescence intensity at 350 nm: ConA incubated with different concentrations (0 to 1500 μM) of gemini G5 (-■-) and G6 (-●-) surfactant at pH 7.4. The ConA concentrations were taken 0.2 mg ml^{-1} in all the measurements. The samples were incubated overnight at room temperature before the measurements.

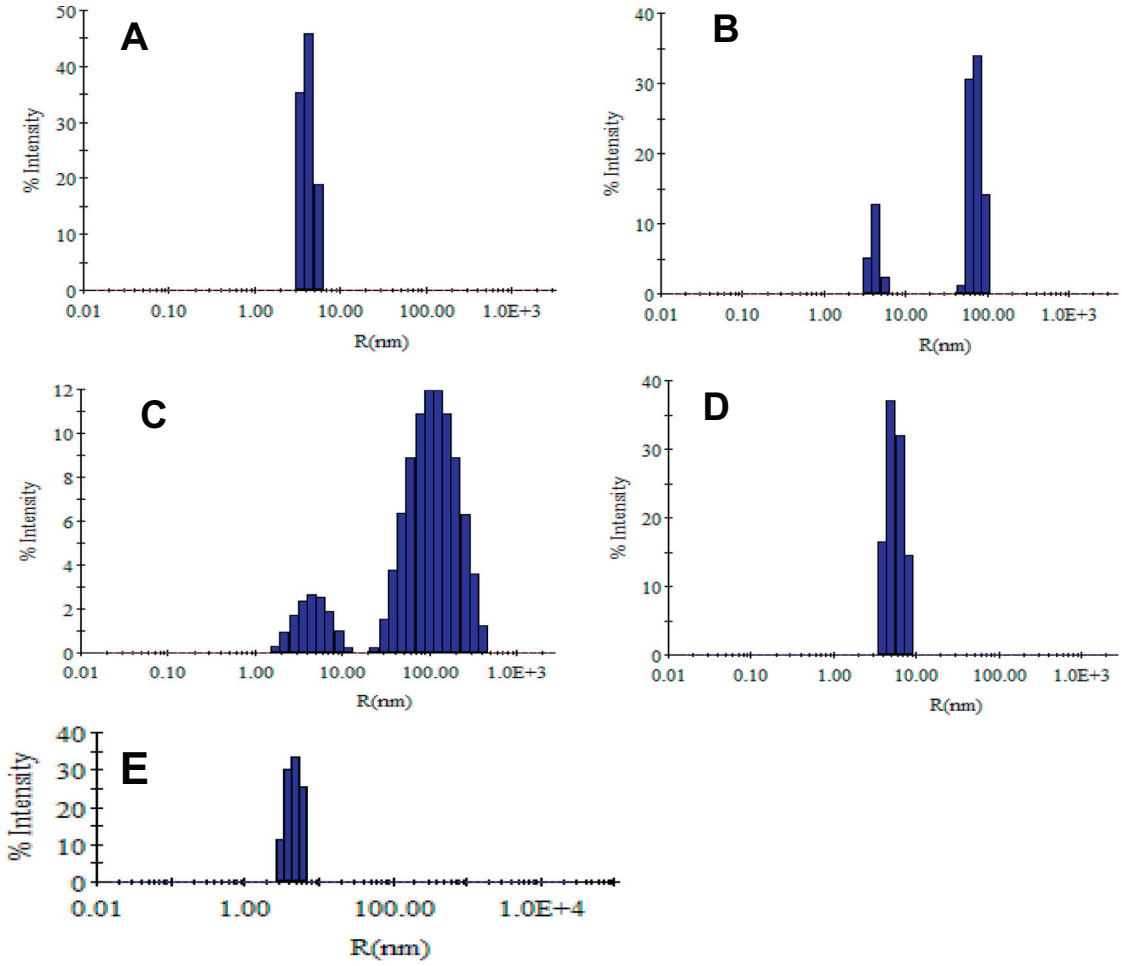

Fig. 3. Hydrodynamic radii of ConA alone (A), in the presence of 50 μM of G5 (B), G6 (C), 500 μM G5 (D) and 500 μM G6 (E) at pH 7.4. ConA concentration was 1.0 mg ml^{-1} in all conditions.

control, the light scattering was not seen in whole the gemini concentrations the data are not shown.

3.3. DLS analysis

DLS is exploited to investigate the hydrodynamic radii of protein and protein aggregates in solution [31]. The modification in the hydrodynamic radii (*Rh*) of ConA in their native states (pH 7.4) and in the presence of 50.0 μM G5 and G6 were measured by DLS (Fig. 3). The *Rh* of ConA at pH 7.4 was found to be 4.3 nm. But, it drastically increased in the presence of 50 μM surfactant (Table 1). Two types of species were found with *Rh* 4.7 and 74.1 nm with 50 μM G5, and 4.9, 112.5 nm with G6 respectively. The first *Rh* clearly represents the monomeric form, but the later one reports polymerization. G6 seems induce larger size aggregates in comparison to G5. But, at 250 μM surfactant concentration, only one species was observed with *Rh* comparable to the ConA monomer. Thus it further suggests disappearance of aggregates at 250 μM surfactants.

3.4. ThT fluorescence assay

Various biophysical techniques are now available to distinguish the morphology of aggregates [32]. Among the highly advance biophysical tools ThT dye is highly used techniques to identified amyloid morphology [33]. ThT form micelles above 4.0 μM and become self-fluorescent at or above 5 μM [34]. ThT micelles specifically bind to the β-sheet and cross-β sheet structure of aggregates and shows huge fluorescence signals compared to unbound ThT [35]. To confirm the morphology of gemini-induced aggregates, ThT dye binding assay was performed. ThT is a cationic benzothiazole dye, known to specifically bind to cross-β structures that exclusively found in amyloid fibrils, and produce increased fluorescence emission around 482 nm [36]. ThT fluorescence

Table 1
Hydrodynamic radii of ConA in the absence and of presence both the gemini surfactant (G5 and G6) at different conditions.

S. No.	Conditions	Hydrodynamic radii (*Rh* (nm))	Polydispersity
1	ConA + pH 7.4	4.3	13.2
2	ConA + 50.0 μM G5 + pH 7.4	4.7, 74.1	20.43, 60.61
3	ConA + 50.0 μM G6 + pH 7.4	4.9, 112.5	28.12, 35.43
4	ConA + 500 μM G5 + pH 7.4	4.8	9.28
5	ConA + 500 μM G6 + pH 7.4	4.9	8.94

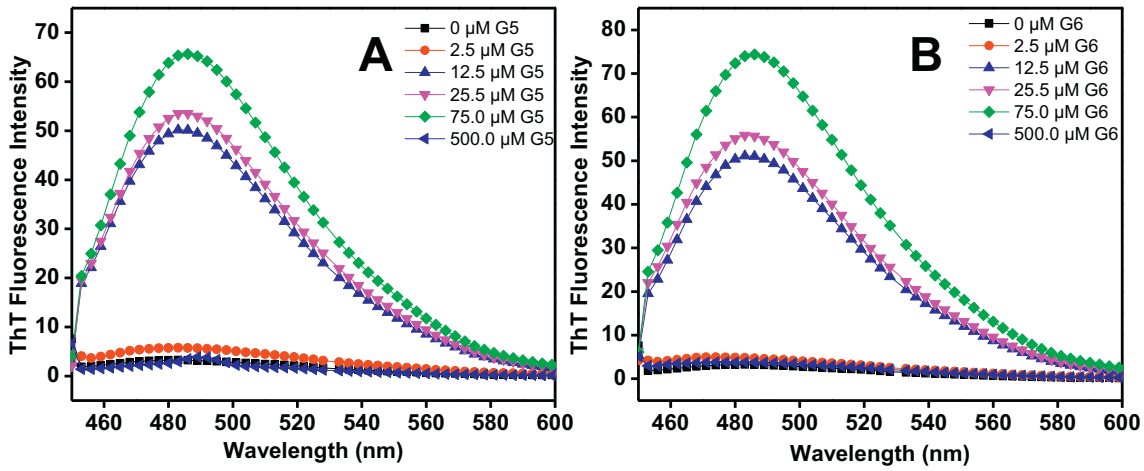

Fig. 4. Thioflavin T (ThT) fluorescence spectra of ConA (0.2 mg ml^{-1}) with respect to increasing concentration of gemini (A) G5 and (B) G6 surfactants at pH 7.4. ThT concentration was taken 5.0 μM in all the samples.

assay of ConA was performed without and with increasing concentrations of G5 (Fig. 4A) and G6 (Fig. 4B) gemini surfactants at pH 7.4. No ThT fluorescence was found in the sample containing ConA without, and with 2.5 and 500.0 μM gemini surfactants. However, ConA with 12.5, 25.0 and 75.0 μM gemini showed huge increase in fluorescence intensity at 482 nm. The results show, ConA formed amyloid-like aggregates at low surfactant concentrations, but aggregates disappeared at and beyond 250 μM concentration.

3.5. Secondary structure transformation determination

Far UV-CD spectroscopy was done to study the changes in secondary structure of ConA with surfactants. The effect of G5 and G6 gemini surfactant on ConA were shown in Fig. 5A and B respectively. It is evident from the figure that the native ConA showed single minima at 218 nm which is characteristic features of β-sheet structure [14]. The negative minima at 218 nm of native ConA was shifted towards higher wavelength in the presence of low concentrations (12.5, 25.0, 37.5, 50.0 and 75.0 μM) of G5 and G6 gemini surfactants and generate new single negative minima around 222 nm. However, in the presence of higher concentrations (250 and 500 μM) of G5 and G6 gemini surfactant, the single negative minima at 218 nm was disappeared and generate two new negative minima i.e., 208 and 222 nm; a characteristic feature of α-helical proteins [37]. The changes in α-helix and β-sheet structures of ConA with surfactant concentration were expressed in Table 2. The CD results clearly show that amyloid state ConA was predominantly β-sheet structure, but at and above 250 μM surfactant concentrations a non-native α-helical structure emerges with the disappearance of aggregation. This may have happened due to local intra-molecular hydrogen bonding.

3.6. Atomic force microscopy measurements

The morphologies of gemini-induced aggregates of ConA protein was studied by atomic force microscopy (AFM). AFM is highly advance-imaging techniques and used to differentiate between amyloid and non-amyloid structure of protein aggregates. AFM images of ConA in the presence of G5 and G6 gemini concentrations (50 μM) at pH 7.4 are shown in Fig. 6A and B. ConA formed amyloid-like fibril with G5 and G6 gemini surfactants, with identical morphologies (long and straight). The diameter of amyloid fibrils formed in the presence of G6 is more compared to the diameter formed in the presence of G5 gemini surfactants. The AFM result further supports that the G5 and G6 treated ConA samples have amyloid-like aggregates.

4. Discussion

Generally, surfactants are promoting amyloid fibrillation in both neurodegenerative and non-neurodegenerative disease related proteins [38–40]. The purpose of this work is to investigate the role of G5

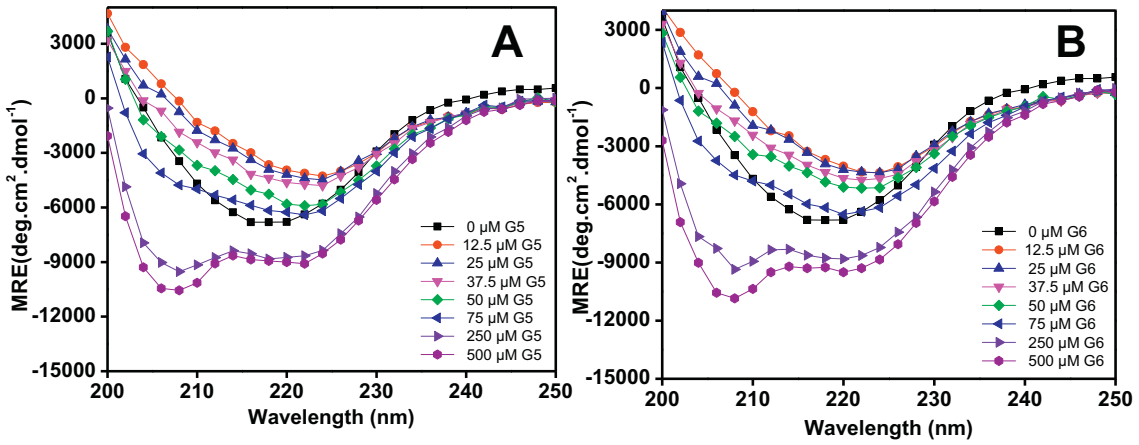

Fig. 5. The far-UV CD spectra of ConA with respect to increasing concentration of gemini (A) G5, (B) G6 surfactant at pH 7.4. The ConA concentrations were taken 0.2 mg ml^{-1}. The gemini treated samples were incubated overnight at room temperature.

Table 2
Percent secondary structure content in ConA protein in response to different concentrations of both the gemini (G5 and G6) surfactant at physiological pH.

S. No.	Conditions	G5		G6	
		% α-helix	% β-sheet	% α-helix	% β-sheet
1	ConA at pH 7.4	9.65	38.75	9.65	38.75
2	ConA at pH 7.4 + 12.5 μM gemini	6.56	42.53	6.56	42.53
3	ConA at pH 7.4 + 25.0 μM gemini	4.49	43.69	5.65	44.57
4	ConA at pH 7.4 + 37.5 μM gemini	5.3	43.19	5.61	44.35
5	ConA at pH 7.4 + 50.0 μM gemini	9.65	43.19	5.10	44.72
6	ConA at pH 7.4 + 75.0 μM gemini	8.11	44.00	4.82	45.45
7	ConA at pH 7.4 + 250.0 μM gemini	26.44	17.4	27.65	24.62
8	ConA at pH 7.4 + 500.0 μM gemini	28.50	16.17	29.87	19.54

and G6 gemini surfactants in the amyloid fibrillation of a carbohydrate binding protein; ConA. In a water/single-chain surfactant biphase, micelles form to minimize its free energy by bringing together the hydrophobic chains by minimizing contact with polar water. The polar head groups remain facing towards water and apart from each other by electrostatic repulsion [41,42].

In gemini surfactants, two head groups chemically linked by a non-polar bridge, and its length and flexibility will remain deciding factor for the surfactant's cmc [43]. With increase in concentration, gemini surfactants first become pre-micellar bodies from monomer, and then become elliptical, cylindrical and lamellar or netlike structure [44]. Near and below the cmc, premicellar start to generate and grow into micelles as the concentration increases [45]. Micelle formation is a multi-step and gradual process [46]. Molecular thermodynamic description of micellization in aqueous medium can be utilized to model self-assembly [47].

The cmc of G5 [47] and G6 gemini surfactants are ~36 to 48 μM [48], while that of CTAB is 920–1000 μM [14]. In the beginning of micellization of surfactants, ConA probably get unfolded and polymerize as reported by turbidity, thioflavin T and polydispersity studies. However, around 250 μM of surfactants, higher degree of micellization may have resulted in the regaining of secondary structures in ConA. Interestingly, due to the solvent engineering of micelles, internalization of hydrogen bonding takes place in ConA, and instead of native β-sheet structures non-native α-helix forms.

ConA (pI = 5.4) is a net negatively charged protein at pH 7.4 [49], so get neutralized even in the presence of a small quantity of cationic surfactants. Thus, in the absence of electrostatic repulsion hydrophobic tail-groups of surfactants will start disrupting hydrophobic pockets of the protein [49]. On further increase of surfactant concentrations tail-groups should start assembling, leaving hydrophobic patches of the protein to form inter-molecular interaction instead of retreating to hydrophobic pocket formation. This state should remain till micellization do not reach to such a higher degree that it starts interfering in the protein's inter-molecular hydrophobic interactions. At higher concentrations, surfactants assemble as vesicle, lamellar or net-like entrapment, instead of solid micelle. Such structures exclude water, which should disintegrate ConA aggregates due to increased presence of electrostatic interaction. Thus, inter-protein hydrophobic interactions get weak, and again monomer start forming. With the increased absence of protein-solvent hydrogen bonding, intra-protein hydrogen bonding takes over, resulting in the formation of non-native alpha helical structures.

From the turbidity and Rayleigh scattering, we have observed that G5 and G6 gemini surfactants, especially in the concentrations range (7.5 to 125 μM), induces aggregation in ConA protein and beyond 250 μM of gemini surfactant ConA aggregation disappear. This is in good agreements with other published reports that low concentrations of surfactant promoted aggregation in protein and higher concentrations of the surfactant demoted the aggregation in proteins [50]. The interesting observation is seen in both the turbidity and light scattering measurements. The turbidity and light scattering found more in the presence of G6 compared to G5 gemini surfactant due to high hydrophobicity. The possible cause of more turbidity and light scattering is due to spacer length of gemini. Over all hydrophobicity of G6 gemini is more compared to G5. More the spacer length having more binding property and simultaneously inducing bigger size aggregates. The hydrodynamic radii (*Rh*) of proteins increase enormously during aggregation [51]. ConA also forms aggregates in the presence of gemini

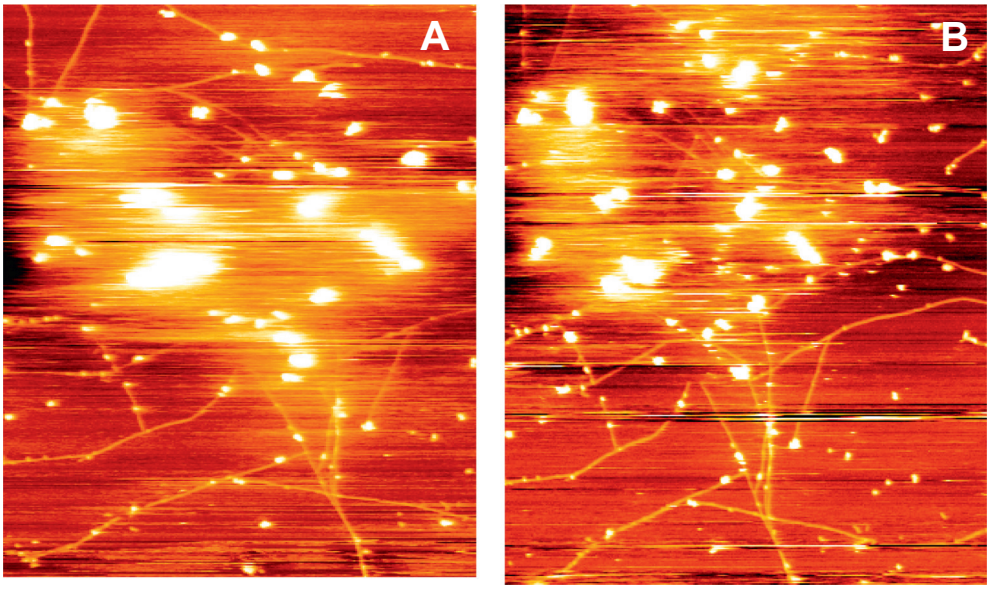

Fig. 6. Atomic force microscopic images of (A) ConA at pH 7.4 + 75.0 μM G5, (B) ConA at pH 7.4 + 75.0 μM G6. ConA concentration was taken 0.2 mg ml^{-1}.

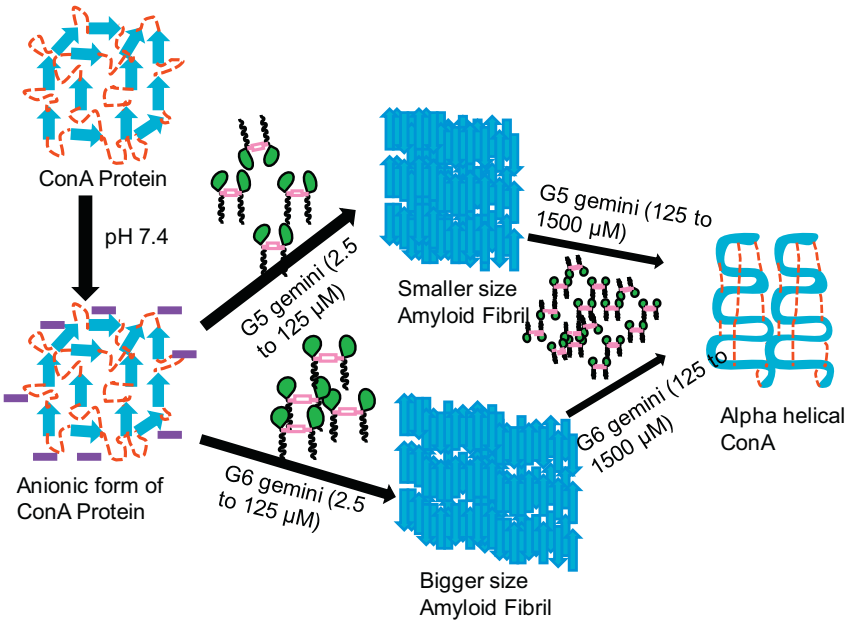

Fig. 7. Schematic representation of effects of G5 and G6 gemini surfactants on ConA protein at pH 7.4.

surfactant, with higher *Rh*. Interestingly, the *Rh* of G6 induced-aggregates was found higher compared to G5 induced-aggregates. The role of spacer length in gemini surfactants on the *Rh* of aggregates is a matter of investigation. Generally, it was seen that the binding efficiency of gemini surfactant reduce with increase in spacer length [52]. It is well-known that aggregation of protein is mostly dependent on hydrophobic and electrostatic interaction [53,54]. The gemini surfactant-induced aggregate morphology was further characterized. ThT has shown positive interaction in the presence of ConA and the gemini surfactant. Gemini-induced aggregates have very high ThT fluorescence confirming that gemini-induced aggregates have amyloid-like structure. The ThT binding was found almost 10 times more in gemini-induced aggregate samples. The positive ThT binding was also found when human and hen egg white lysozyme was incubated at pH 1.5 and higher temperature [35]. For more detail characterization, AFM imaging was done to identify the morphology of gemini-induced ConA aggregates. The AFM image showed that the ConA form long and straight fibril and the diameter were found bigger in the presence of G6 gemini surfactant.

Amyloid fibrils make cross-β sheet structure that is difficult to distinguish from β sheet structures by far-UV CD measurements. Recently, it was reported that hyperthermophile protein from amyloid-like aggregates in the presence of low SDS concentrations and amyloid fibril have a cross-β sheet structure [55]. The native ConA poses 38.75% β-sheet structure that is similar to already published reports [56]. The negative ellipticity was found to reduce in the presence of low concentrations of G5 and G6 gemini surfactant along with increase in β-structure. On the contrary, the percent α-helix increased in the presence of higher G5 and G6 gemini surfactant. Alcohols, predominantly 2,2,2 trifuloroethanol (TFE), have been reported to induce α-helices in β-sheet proteins. There are very few reports of β-sheet to α-helix transition induced by non-alcoholic substances. Our lab is pioneer in reporting surfactant (CTAB) induced β-sheet to α-helix transition in ConA [14]. A 25 amino acid domain Bax-alpha1 found to show β-sheet to α-helix upon interaction with negatively charged phospholipid vesicles [57]. Zhu and Fink have reported that the α-helical conformation induced by the anionic lipid vesicles is not fibrillogenic [58]. First G5 and G6 gemini surfactant induced β-sheet to α-helix transition has been observed. ConA being apoptotic to cancerous cells [59], and having potential therapeutic effect on hepatoma [60], the observations done in this work could be of immense interest in vesicular delivery of ConA. Lectin (ConA, RGA and WGA)-Fe_3O_4 silver nanoparticle has been successfully used for MR and CT imaging in-vitro and colorectal cancer in-vivo [61]. ConA has been found to induce caspase dependent apoptosis in human melanoma A375 cells. ConA inhibits hepatic metastasis of colon-26 cells through NK-mediated mechanism, B-16 melanoma cells and fibroblast 3T3 cells [62–64].

The detail mechanism of amyloid fibril formation in ConA is presented in schematic diagram shown in Fig. 7. The ConA exist in anionic form at physiological pH, the low concentrations of gemini surfactant induces amyloid-like fibrils at physiological. The positively charged head group of G5 and G6 gemini surfactants are interacted electrostatically to aspartic and glutamic acid of ConA protein and neutralize the charges and similarly, hydrophobic tail is breaking down solvent ConA interaction, which is leading to amyloid fibril formation. However, higher concentrations of gemini surfactants are inducing alpha helical structure in ConA protein.

5. Conclusion

In this study, we have concluded that G5 and G6 gemini surfactants (7.5 to 125 μM) induces amyloid fibril in ConA lectin at physiological pH 7.4. However, in the presence 250 μM and above concentrations of these surfactants aggregates disappear, and β-sheet to α-helix transition takes place. The spacer length is also playing important role in aggregation of ConA. The turbidity, light scattering and *Rh* is registered in the amyloid fibrils made with same concentration of G5 and G6 but the turbidity, light scattering and *Rh* is found more in the presence of G6 gemini surfactant. The observations are of immense importance as this is one of the first reports of β-sheet to α-helix transition with detergents, that to with an intermittent amyloid formation. Further studies may clarify the mechanism of the β-sheet to α-helix transition and its exploitation in the vesicular or liposomal packing of ConA for targeted delivery. Although, there is number of reports of β-sheet to α-helix transition at non-physiological temperature, but such circumstances are difficult to induce in tumor cells. The effectiveness of gemini at such a low concentration, could be potentially exploited in ConA mediated therapies.

Supplementary data to this article can be found online at https://doi.org/10.1016/j.molliq.2018.08.092.

Acknowledgements

The authors extend their appreciation to the Deanship of Scientific Research at King Saud University for funding the work through the research group project No. RG-1437-004.

References

[1] D. Eisenberg, M. Jucker, The amyloid state of proteins in human diseases, Cell 148 (2012) 1188–1203.
[2] J.D. Sipe, M.D. Benson, J.N. Buxbaum, S. Ikeda, G. Merlini, M.J.M. Saraiva, P. Westermark, Nomenclature 2014: amyloid fibril proteins and clinical classification of the amyloidosis, Amyloid 21 (2014) 221–224.
[3] J.D. Sipe, A.S. Cohen, Review: history of the amyloid fibril, J. Struct. Biol. 130 (2000) 88–98.
[4] R.N. Rambaran, L.C. Serpell, Amyloid fibrils: abnormal protein assembly, Prion 2 (2008) 112–117.
[5] M. Fändrich, V. Forge, K. Buder, M. Kittler, C.M. Dobson, S. Diekmann, Myoglobin forms amyloid fibrils by association of unfolded polypeptide segments, Proc. Natl. Acad. Sci. U. S. A. 100 (2003) 15463–15468.
[6] V.K. Sharma, D.S. Kalonia, Temperature- and pH-induced multiple partially unfolded states of recombinant human interferon-alpha2a: possible implications in protein stability, Pharm. Res. 20 (11) (2003) 1721–1729.
[7] C.C. Lee, A. Nayak, A. Sethuraman, G. Belfort, G.J. McRae, A three-stage kinetic model of amyloid fibrillation, Biophys. J. 92 (2007) 3448–3458.
[8] S. Shamsi, R.H. Hidayathulla, Khan, Negatively charged food additive dye "Allura Red" rapidly induces SDS-soluble amyloid fibril in beta-lactoglobulin protein, Int. J. Biol. Macromol. 107 (2018) 1706–1716.
[9] M. Nors Perdersen, V. Foderà, I. Horvath, A. van Maarschalkerweerd, K. Nørgaard Toft, C. Weise, F. Almqvist, M. Wolf-Watz, P. Wittung-Stafshede, B. Vestergaard, Direct correlation between ligand-induced α-synuclein oligomers and amyloid-like fibril growth, Sci. Rep. 5 (2015) 10422.
[10] T. Matsubara, M. Nishihara, H. Yasumori, M. Nakai, K. Yanagisawa, T. Sato, Size and shape of amyloid fibrils induced by ganglioside nanoclusters: role of sialyl oligosaccharide in fibril formation, Langmuir 33 (48) (2017) 13874–13881.
[11] H.M. Swasthi, S. Mukhopadhyay, Electrostatic lipid-protein interactions sequester the curli amyloid fold on the lipopolysaccharide membrane surface, J. Biol. Chem. 292 (48) (2017) 19861–19872.
[12] S.K. Chaturvedi, J.M. Khan, M.K. Siddiqi, P. Alam, R.H. Khan, Comparative insight into surfactants mediated amyloidogenesis of lysozyme, Int. J. Biol. Macromol. 83 (2016) 315–325.
[13] J.M. Khan, M.S. Khan, M.A. Alsenaidy, A. Ahmed, P. Sen, M. Oves, N.A. Al-Shabib, R.H. Khan, Sodium louroyl sarcosinate (sarkosyl) modulate amyloid fibril formation in hen egg white lysozyme (HEWL) at alkaline pH: a molecular insight study, J. Biomol. Struct. Dyn. (2017) 1–16, https://doi.org/10.1080/07391102.2017.1329097.
[14] J.M. Khan, M.S. Khan, M.S. Ali, N.A. Al-Shabib, R.H. Khan, Cetyltrimethylammonium bromide (CTAB) promote amyloid fibril formation in carbohydrate binding protein (concanavalin A) at physiological pH, RSC Adv. 6 (2016) 38100–38111.
[15] M. Zaman, S.M. Zakariya, S. Nusrat, M.V. Khan, A. Qadeer, M.R. Ajmal, R.H. Khan, Surfactant-mediated amyloidogenesis behavior of stem bromelain; a biophysical insight, J. Biomol. Struct. Dyn. 35 (7) (2017) 1407–1419.
[16] M. Cao, Y. Han, J. Wang, Y. Wang, Modulation of fibrillogenesis of amyloid beta (1–40) peptide with cationic gemini surfactant, J. Phys. Chem. B 111 (47) (2009) 13436–13443.
[17] F.M. Menger, C.A. Littau, Gemini surfactants: a new class of self-assembling molecules, J. Am. Chem. Soc. 115 (22) (1993) 10083–10090.
[18] Y. Li, X. Wang, Y. Wang, Comparative studies on interactions of bovine serum albumin with cationic gemini and single-chain surfactants, J. Phys. Chem. B 110 (16) (2006) 8499–8505.
[19] F.M. Menger, J.S. Keiper, V. Azov, Gemini surfactants with acetylenic spacers, Langmuir 16 (5) (2000) 2062–2067.
[20] D. Kumar, M.A. Rub, Kinetic study of nickel-glycylglycine with ninhydrin in alkanediyl α,ω gemini (m-s-m type) surfactant system, J. Mol. Liq. 240 (2017) 253–257.
[21] D. Kumar, M.A. Rub, Effect of anionic surfactant and temperature on micellization behavior of promethazine hydrochloride drug in absence and presence of urea, J. Mol. Liq. 238 (2017) 389–396.
[22] R. Sabaté, J. Estelrich, Stimulatory and inhibitory effects of alkyl bromide surfactants on beta-amyloid fibrillogenesis, Langmuir 21 (15) (2005) 6944–6949.
[23] A.R. Amin, R.K. Paul, V.S. Thakur, M.L. Agarwal, Novel role for p73 in the regulation of Akt-Foxo1a-Bim signaling and apoptosis induced by the plant lectin, concanavalin A, Cancer Res. 67 (2007) 5617–5620.
[24] J. Becker, G.J. Reeke, J. Wang, B. Cunningham, G. Edelman, The covalent and three-dimensional structure of concanavalin A. III. Structure of the monomer and its interactions with metals and saccharides, J. Biol. Chem. 250 (1975) 1513–1524.
[25] V. Vetri, F. Librizzi, V. Militello, M. Leone, Effects of succinylation on thermal induced amyloid formation in concanavalin A, Eur. Biophys. J. 36 (2007) 733–741.
[26] N. Mitra, V.R. Srinivas, T.N.C. Ramya, N. Ahmad, G.B. Reddy, A. Surolia, Conformational stability of legume lectins reflect their different modes of quaternary association: solvent denaturation studies on concanavalin A and winged bean acidic agglutinin, Biochemistry 41 (2002) 9256–9263.
[27] J. Emsely, H.E. White, B.P. OHara, G. Oliva, N. Srinivasan, I.J. Tickle, T.L. Blundell, M.B. Pepys, S.P. Wood, Structure of pentameric human serum amyloid P component, Nature 367 (1994) 338–345.
[28] R. Carrotta, V. Vetri, F. Librizzi, V. Martorana, V. Militello, M. Leone, Amyloid fibrils formation of concanavalin A at basic pH, J. Phys. Chem. B 115 (12) (2011) 2691–2698.
[29] V. Vetri, F. Librizzi, M. Leone, V. Militello, Thermal aggregation of bovine serum albumin at different pH: comparison with human serum albumin, Eur. Biophys. J. 36 (7) (2007) 717–725.
[30] W. Fatma Kabir-ud-Din, Z.A. Khan, A.A. Dar, H NMR and viscometric studies on cationic gemini surfactants in presence of aromatic acids and salts, J. Phys. Chem. B 111 (2007) 8860–8867.
[31] S. Kumar, J.B. Udgaonkar, Conformational conversion may precede or follow aggregate elongation on alternative pathways of amyloid protofibril formation, J. Mol. Biol. 385 (4) (2009) 1266–1276.
[32] M. Biancalana, S. Koide, Molecular mechanism of thioflavin-t binding to amyloid fibrils, Biochim. Biophys, Acta. 1804 (7) (2010) 1405–1412.
[33] Li Huiyuan, F. Rahimi, S. Sinha, P. Maiti, G. Bitan, K. Murakami, in: R.A. Meyers (Ed.), Amyloids and Protein Aggregation—Analytical Methods. Encyclopedia of Analytical Chemistry, John Wiley & Sons Ltd, 2009https://doi.org/10.1002/9780470027318.a9038.
[34] P.S. Vassar, C.F. Culling, Fluorescent stains, with special reference to amyloid and connective tissues, Arch. Pathol. 68 (1959) 487–498.
[35] C. Xue, T.Y. Lin, D. Chang, Z. Guo, Thioflavin T as an amyloid dye: fibril quantification, optimal concentration and effect on aggregation, R. Soc. Open Sci. 4 (1) (2017), 160696.
[36] R. Khurana, C. Coleman, C. Ionescu-Zanetti, S.A. Carter, V. Krishna, R.K. Grover, R. Roy, S. Singh, Mechanism of thioflavin T binding to amyloid fibrils, J. Struct. Biol. 151 (2005) 229–238.
[37] M.A. Rub, J.M. Khan, N. Azum, A.M. Asiri, Influence of antidepressant clomipramine hydrochloride drug on human serum albumin: spectroscopic study, J. Mol. Liq. 241 (2017) 91–98.
[38] M.A. Alsenaidy, Biophysical evaluation of amyloid fibril formation in bovine cytochrome *c* by sodium lauroyl sarcosinate (sarkosyl) in acidic conditions, J. Mol. Liq. 241 (2017) 722–729.
[39] H.M. Saunders, V.A. Hughes, R. Cappai, S.P. Bottomley, Conformational behavior and aggregation of ataxin 3 in SDS, PLoS One 8 (7) (2013), e69416.
[40] K. Yamaguchi, H. Naiki, Y. Goto, Mechanism by which the amyloid-like fibrils of beta 2 microglobulin fragment are induced by fluorine-substituted alcohols, J. Mol. Biol. 363 (2006) 279–288.
[41] M.A. Rub, N. Azum, A.M. Asiri, Binary mixtures of sodium salt of ibuprofen and selected bile salts: interface, micellar, thermodynamic, and spectroscopic study, J. Chem. Eng. Data 62 (2017) 3216–3228.
[42] M.A. Rub, N. Azum, F. Khan, A.M. Asiri, Aggregation of sodium salt of ibuprofen and sodium taurocholate mixture in different media: a tensiometry and fluorometry study, J. Chem. Thermodyn. 121 (2018) 199–210.
[43] S. Karaborni, K. Esselink, P.A. Hilbers, B. Smit, J. Karthauser, N.M. van Os, R. Zana, Simulating the self-assembly of gemini (dimeric) surfactants, Science 266 (5183) (1994) 254–256.
[44] X. Cui, S. Mao, M. Liu, H. Yuan, Y. Du, Mechanism of surfactant micelle formation, Langmuir 24 (19) (2008) 10771–10775.
[45] F. Khan, U.S. Siddiqui, M.A. Rub, I.A. Khan, Kabir-ud-Dinb, Micellization and interfacial properties of cationic gemini surfactant (12–4–12) in the presence of additives in aqueous electrolyte solution: a tensiometric study, J. Mol. Liq. 191 (2014) 29–36.
[46] N. Azum, M.A. Rub, A.M. Asiri, Interaction of triblock-copolymer with cationic gemini and conventional surfactants: a physicochemical study, J. Dispers. Sci. Technol. 38 (2017) 1785–1791.
[47] M.A. Rub, N. Azum, F. Khan, A.M. Asiri, Surface, micellar, and thermodynamic properties of antidepressant drug nortriptyline hydrochloride with TX-114 in aqueous/urea solutions, J. Phys. Org. Chem. 30 (2017), e3676.
[48] A. Abelein, J.D. Kaspersen, S.B. Nielsen, G.V. Jensen, G. Christiansen, J.S. Pedersen, J. Danielsson, D.E. Otzen, A. Gräslund, Formation of dynamic soluble surfactant-induced amyloid β peptide aggregation intermediates, J. Biol. Chem. 288 (32) (2013) 23518–23528.
[49] J.M. Khan, A. Qadeer, S.K. Chaturvedi, E. Ahmad, S.A. Rehman, S. Gourinath, R.H. Khan, SDS can be utilized as an amyloid inducer: a case study on diverse proteins, PLoS One 7 (1) (2012), e29694.
[50] J.M. Khan, S.K. Chaturvedi, S.K. Rahman, M. Ishtikhar, A. Qadeer, E. Ahmad, R.H. Khan, Protonation favors aggregation of lysozyme with SDS, Soft Matter 10 (15) (2014) 2591–2599.
[51] M.F. Ahmad, T. Ramakrishna, B. Raman, Ch.M. Rao, Fibrillogenic and non-fibrillogenic ensembles of SDS-bound human α-synuclein, J. Mol. Biol. 364 (2006) 1061–1072.
[52] M.A. Mir, J.M. Khan, R.H. Khan, G.M. Rather, A.A. Dar, Effect of spacer length of alkanediyl-alpha, omega-bis (dimethylcetylammonium bromide) geminihomologues on the interfacial and physicochemical properties of BSA, Colloids Surf. B: Biointerfaces 77 (1) (2010) 54–59.
[53] J.M. Khan, S.A. Abdulrehman, F.K. Zaidi, S. Gourinath, R.H. Khan, Hydrophobicity alone cannot trigger aggregation in protonated mammalian serum albumins, Phys. Chem. Chem. Phys. 16 (11) (2014) 5150–5161.
[54] N.A. Al-Shabib, J.M. Khan, M.A. Alsenaidy, A.M. Alsenaidy, M.S. Khan, F.M. Husain, M.R. Khan, M. Naseem, P. Sen, P. Alam, R.H. Khan, Unveiling the stimulatory effects of tartrazine on human and bovine serum albumin fibrillogenesis: spectroscopic and microscopic study, Spectrochim. Acta A Mol. Biomol. Spectrosc. 191 (2018) 116–124.
[55] J.M. Khan, P. Sharma, K. Arora, N. Kishor, P. Kaila, P. Guptasarma, The Achilles' heel of "ultrastable" hyperthermophile proteins: submillimolar concentrations of SDS stimulate rapid conformational change, aggregation, and amyloid formation in proteins carrying overall positive charge, Biochemistry 55 (28) (2016) 3920–3936.

[56] M.J. Swamy, M.V.K. Sastry, A. Surolia, Prediction and comparison of the secondary structure of legume lectins, J. Biosci. 9 (1985) 203–212.
[57] M.A. Sani, C. Loudet, G. Gröbner, E.J. Dufourc, Pro-apoptotic bax-alpha1 synthesis and evidence for beta-sheet to alpha-helix conformational change as triggered by negatively charged lipid membranes, J. Pept. Sci. 13 (2) (2007) 100–106.
[58] M. Zhu, A.L. Fink, Lipid binding inhibits α-synuclein fibril formation, J. Biol. Chem. 278 (19) (2003) 16873–16877.
[59] F.F. Becker, A. Shurgin, Concanavalin A agglutination of cells from primary hepatocellular carcinomas and hepatic nodules induced by *N* 2 fluorenylacetamide, Cancer Res. 35 (10) (1975) 2879–2883.
[60] H.Y. Lei, C.P. Chang, Lectin of Concanavalin A as an anti-hepatoma therapeutic agent, J. Biomed. Sci. 16 (2009) 10.
[61] X. He, F. Liu, L. Liu, T. Duan, H. Zhang, Z. Wang, Lectin-conjugated Fe_2O_3@Au core@shell nanoparticles as dual mode contrast agents for in vivo detection of tumor, Mol. Pharm. 11 (3) (2014) 738–745.
[62] C.Y. Li, H.L. Xu, B. Liu, J.K. Bao, Concanavalin A, from an old protein to novel candidate anti-neoplastic drug, Curr. Mol. Pharmacol. 3 (3) (2010) 123–128.
[63] H.Y. Lei, C.P. Chang, Induction of autophagy by concanavalin A and its application in anti-tumor therapy, Autophagy 3 (4) (2007) 402–404.
[64] J. Pratt, R. Roy, B. Annabi, Concanavalin-A-induced autophagy biomarkers requires membrane type-1 matrix metalloproteinase intracellular signaling in glioblastoma cells, Glycobiology 22 (9) (2012) 1245–1255.